Nuclear Inst. and Methods in Physics Research, A 912 (2018) 177–181

Contents lists available at ScienceDirect

Nuclear Inst. and Methods in Physics Research, A

journal homepage: www.elsevier.com/locate/nima

Evaluation of silicon photomultipliers for dual-mirror Small-Sized Telescopes of Cherenkov Telescope Array

A. Asano [a], D. Berge [b], G. Bonanno [c], M. Bryan [b], B. Gebhardt [d], A. Grillo [c], N. Hidaka [a], P. Kachru [b], J. Lapington [e], S. Leach [e], Y. Nakamura [a], A. Okumura [a], G. Romeo [c], D. Ross [e], M. Stephan [b], H. Tajima [a,*], M.C. Timpanaro [c], R. White [d], N. Yamane [a], A. Zink [f], for the CTA Consortium

[a] Institute for Space–Earth Environmental Research, Nagoya University, Nagoya 464-8601, Japan
[b] GRAPPA, University of Amsterdam, 1098 XH Amsterdam, Netherlands
[c] INAF, Osservatorio Astrofisico di Catania, Via S. Sofia 78, I-95123 Catania, Italy
[d] Max-Planck-Institut für Kernphysik, 69029 Heidelberg, Germany
[e] Department of Physics and Astronomy, University of Leicester, Leicester, LE1 7RH, UK
[f] Erlangen Centre for Astroparticle Physics, D-91058, Erlangen, Germany

ARTICLE INFO

Keywords:
Silicon photomultiplier
Photon detector
Gamma ray
Air shower
Cherenkov radiation
Astrophysics

ABSTRACT

All camera designs for Small-Sized telescopes (SSTs) proposed for the Cherenkov Telescope Array (CTA) utilize silicon photomultipliers (SiPM) as their baseline photon sensor technology. The dual-mirror SST (SST-2M) has a smaller plate scale (i.e. image size) than the single-mirror SST, allowing it to employ 2,000 square SiPMs with pixel sizes of approximately 6 mm, close to the mainstream SiPM sizes.

In CTA, the night sky background level of typically ~25 Mcounts/s/pixel (>100 Mcounts/s/pixel at maximum) places severe constraints on the trigger capability due to accidental coincidence on neighboring pixels. In order to suppress such events, it is necessary to reduce optical crosstalk, a mechanism whereby a single optical photon can produce multiple avalanches in the SiPM, while keeping good photon detection efficiency. These are, in general, contradicting requirements.

In this manuscript, we report on characterization of a variety of SiPM technologies for SST-2M cameras and compare results obtained at different participating institutions. We assess the harmonization of results and discuss the likely performance that will be achieved for the first production cameras.

1. Introduction

The Cherenkov Telescope Array (CTA) [1] is a project to build the next generation ground-based gamma-ray observatory, employing three telescope design groupings, the Large, Medium and Small-sized Telescope (SST) arrays to enhance the sensitivity over current facilities by up to an order of magnitude [2] in the 100 GeV to 10 TeV range and extend the accessible energy range from well below 100 GeV to above 100 TeV. The SST array is optimized for sensitivity and coverage from a few TeV to 300 TeV.

We plan to deploy ~ 70 SSTs over an area of several km 2 in order to achieve the sensitivity requirement. Because of the large number of telescopes required, cost reduction is critical for the SST. The cost of the optics is reduced by reducing the size of the telescope. However, the camera cost cannot be reduced by simply shrinking its size, due to the minimum number of pixels required (> 1,000) and the relatively high unit cost of traditional photon sensing photomultiplier tubes. In order to mitigate this problem, the SST utilizes silicon photomultipliers (SiPMs) as the baseline photon sensor technology [3]. Although the unit cost of SiPMs is low (in the order of tens of euros instead of hundreds of euros for phototubes), it is still expensive to cover the entire focal plane of the single-mirror SST design. One solution is to employ a light concentrator in front of each SiPM so that the effective collection area of the SiPM can be expanded, but with some loss of photons. The other solution is to employ dual-mirror optics which have a smaller plate scale (i.e. image size) than the single-mirror SST, allowing them to employ ~

* Corresponding author.
E-mail address: tajima@nagoya-u.jp (H. Tajima).

https://doi.org/10.1016/j.nima.2017.11.017
Received 30 September 2017; Received in revised form 27 October 2017; Accepted 6 November 2017
Available online 13 November 2017

2,000 square SiPMs with pixel sizes of approximately 6 mm, close to the mainstream SiPM sizes.

In this paper, we report on the characterization of a variety of SiPM technologies for dual-mirror SST (SST-2M) cameras, which is being undertaken in parallel within several groups belong to the consortia building CTA SST-2M telescopes.

2. Requirements on photodetectors

In CTA, Cherenkov photons produced by gamma-ray showers are observed which peaks around 350 nm and arrives within a few to a few tens of ns. Because of this, good photon detection efficiency (PDE) at from near UV to blue and ns order timing are important for photodetectors. Since the angular range of the incident photon impinging on the focal plane is 30–60° in the dual-mirror SSTs, the PDEs in these angles are relevant. The greatest challenge for photodetectors in CTA comes from the night sky background (NSB) whose rate is typically ~ 25 Mcounts/s/pixel (> 100 Mcounts/s/pixel at maximum). It peaks above 550 nm and places severe constraints on the trigger capability due to accidental coincidence on neighboring pixels. In order to suppress such events, it is necessary to reduce optical crosstalk (OCT), a mechanism whereby a single incident photon can produce multiple avalanches in the SiPM, while still enhancing the PDE. These are, in general, contradicting requirements.

We have tested a variety of SiPM devices utilizing different technologies from Hamamatsu, FBK and SensL, and of different pixel sizes and individual cell sizes. In this paper, we focus on the test results of Hamamatsu devices due to availabilities of variety of pixel and cell sizes. LCT5 (Low CrossTalk 5th generation) devices from Hamamatsu employ narrow trenches between avalanche cells in order to prevent spread of photons produced by electron–hole pairs in the avalanche while minimizing the loss of the incident photons due to cell gaps. LVR (Low Breakdown Voltage) devices from Hamamatsu employ the same cell structure as LCT5 with a lower breakdown voltage and higher cell capacitance, resulting in higher PDE at a lower over voltage while the OCT rate is still low. (The typical breakdown voltage of LVR devises is 37 V while the breakdown voltage of LCT5 devices is 52 V.) LVR2 has improved optical crosstalks due to optimized manufacturing processes. Table 1 summarizes the specifications of the tested devices.

3. Photon detection efficiency

The PDE is measured by counting the average number of detected photons in coincidence with the pulsed light source (LED or laser) with respect to the number of incident photons. In order to avoid the effect of the OCT, we measure the probability of detecting 0 photons and derive the average assuming the Poisson statistics. The number of incident photon is calibrated using a calibrated photodiode at the Catania site, and using a reference SiPM at the Nagoya site. (Since the absolute PDE of the reference SiPM is calibrated using the Catania measurements, absolute PDE scales of the Catania and Nagoya measurements are not independent.) The effect of dark-noise count is taken into account by repeating the same measurement in the dark condition.

Fig. 1(a) shows the PDE as a function of the over voltage for the wavelength of 405 nm measured at Nagoya. (The PDEs are measured at 405 nm at both sites throughout the paper unless otherwise noted.) We observe some clustering due to cell size and pixel size differences and also due to the technology differences. In order to account for known dependences on the cell fill factor and breakdown voltage, Fig. 1(b) shows the PDE divided by fill factor as a function of the ratio of the over voltage relative to the breakdown voltage. As a result, we find S13360-3050CS gives 5% better PDE than other types of SiPMs and LVR2 devices show 5% worse PDE than other types of SiPMs. The PDE results for S13360-3050CS may be outliers because we do not find any particular reason why this cell size and pixel size combination gives better PDE than others with the same technology. Since we use a collimated light source (the diameter of the light is about 1 mm), difference may arise from the position of the exposure. Some of SiPMs tested at Nagoya site were sent to Catania for verification and PDEs are measured as shown in Fig. 1(c). We do not observe any strong dependence on technologies although we also find two outliers. The fact that most devices follow the same curve indicates that we can estimate the PDE by scaling the fill factor and the relative over voltage.

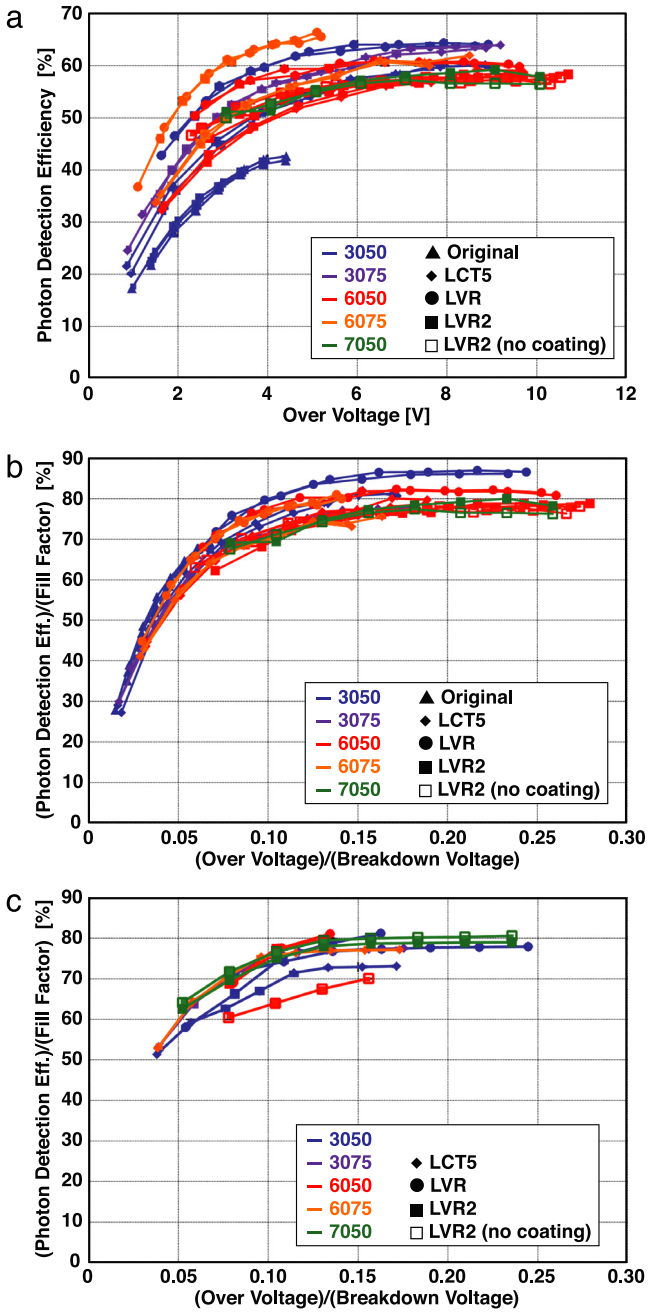

Fig. 1. (a) PDE as a function of the over voltage measured at Nagoya. (b) PDE normalized by the cell fill factor as function of the relative over voltage at Nagoya. (c) PDE normalized by the cell fill factor as function of the relative over voltage at Catania.

Since we prefer photodetectors with good sensitivity in blue-UV region and poor sensitivity in red-IR region, we compared the PDE dependence on the wavelength between LVR and LCT5 at an over voltage of 3 V as shown in Fig. 2. We find that the red sensitivity of LVR is suppressed by 15% than the blue sensitivity compared with LCT5 due to thinner active depth.

Table 1
Summary of specifications for tested SiPMs.

Product ID	Technology	Pixel size (mm)	Cell size (μm)	Cell fill factor	Coating thickness (μm)	Coating material
S12572-050C	Original	3	50	0.62	450	Epoxy
S13360-3050CS	LCT5	3	50	0.74	450	Silicone
S13360-3050VE	LCT5	3	50	0.74	100	Epoxy
S13360-3050PE	LCT5	3	50	0.74	300	Epoxy
S13360-6050CS	LCT5	6	50	0.74	450	Silicone
S13360-3075CS	LCT5	3	75	0.82	450	Silicone
S13360-6075CS	LCT5	6	75	0.82	450	Silicone
LVR-3050CS-SMP	LVR	3	50	0.74	450	Silicone
LVR-6050CS-SMP	LVR	6	50	0.74	450	Silicone
LVR-7050CS-SMP	LVR	7	50	0.74	450	Silicone
LVR-6075CS-SMP	LVR	6	75	0.82	450	Silicone
LVR-6050CS-SMP2	LVR2	6	50	0.74	450	Silicone
LVR-6050CN-SMP2	LVR2	6	50	0.74	N/A	None
LVR-7050CS-SMP2	LVR2	7	50	0.74	450	Silicone
LVR-7050CN-SMP2	LVR2	7	50	0.74	N/A	None

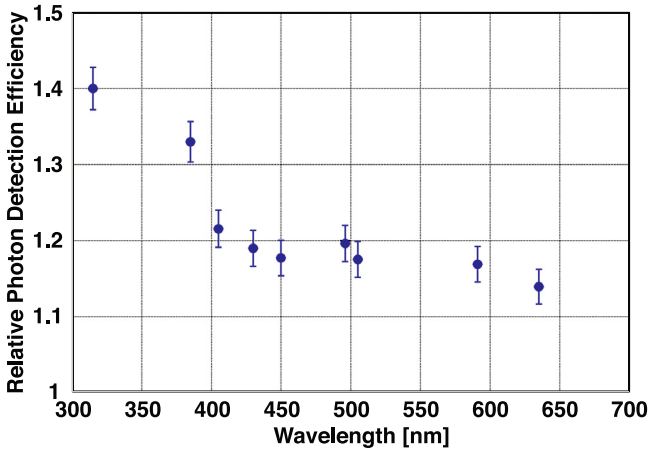

Fig. 2. Relative PDE of LVR with respect to the LCT5 at the over voltage of 3 V as a function of the wavelength measured at Catania.

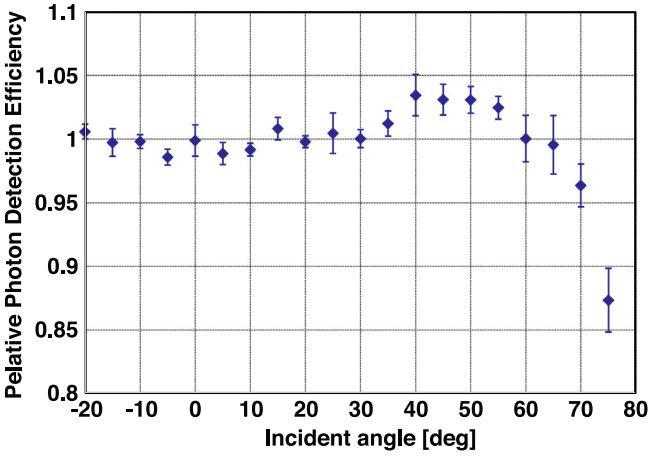

Fig. 3. PDE as a function of the incident angle measured at Catania [4].

Another important requirement on the PDE is angular dependence since the incident photon angle is mostly 30–60° in the dual-mirror SSTs. Fig. 3 shows the PDE dependence on the incident angle measured at the Catania site [4]. We find more or less constant PDE up to 65°.

4. Optical crosstalk

The OCT rate is measured as a fraction of the events with two or more photo-electrons with respect to the number of the dark-noise counts

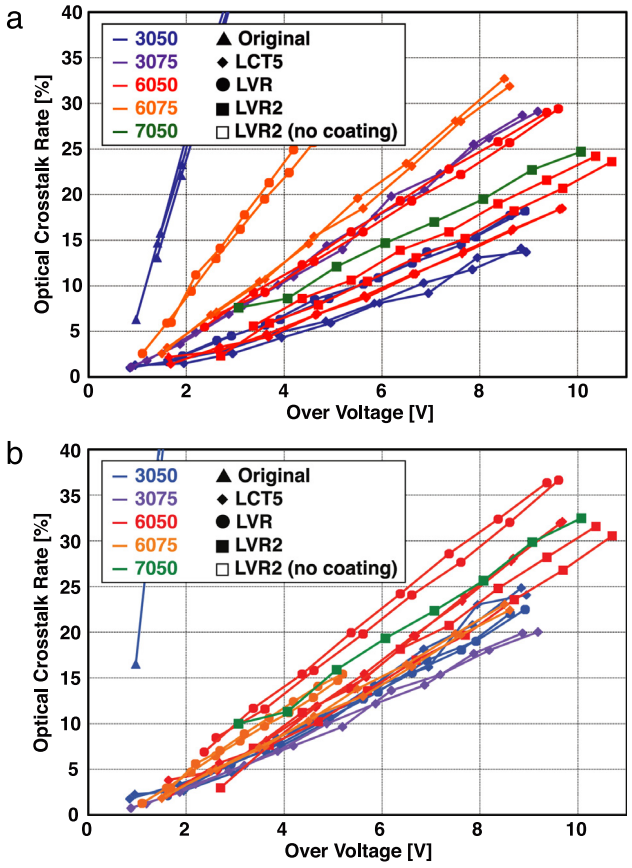

Fig. 4. (a) OCT as a function of the over voltage measured at Nagoya. (b) OCT scaled by the cell area and cell depth as a function of the over voltage measured at Nagoya.

assuming that the dark-noise counts only produce one photo-electron initially. Since the dark-noise count rate can be as high as a few MHz at room temperatures at high over voltages, two photo-electron events due to chance coincidence of two independent dark-noise counts are not negligible. In order to suppress such events, waveforms from SiPMs are digitally recorded with 500 MHz bandwidth and 4 Gsps sampling rate at the Nagoya site and digital filtering are applied with an ability to separate two pulses as short as 5 ns apart. Remaining chance coincidence rate is corrected for using the measured dark-noise count rates. At the Catania site, the OCT is measured using a 15-ns bipolar shaper at a temperature of 2 °C where the chance coincidence of the dark-noise counts is not significant.

Fig. 4(a) shows the OCT rate as a function of the over voltage measured at Nagoya. Since OCT rate depends on many factors, it will

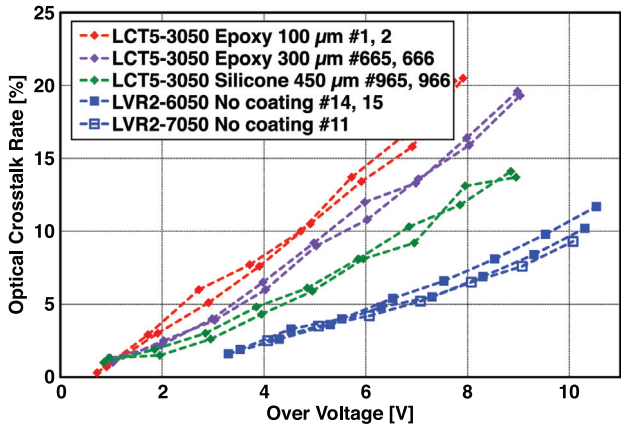

Fig. 5. OCT as a function of the over voltage for SiPMs with different coating thickness measured at Nagoya.

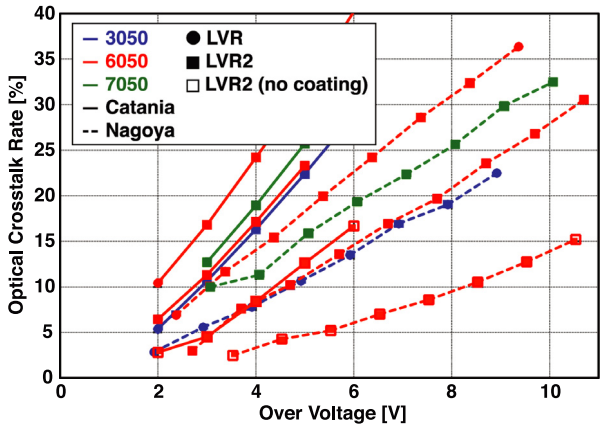

Fig. 6. Comparison of OCT measurements between Nagoya and Catania.

be useful to take out known factors such as cell capacitance. Fig. 4(b) shows the OCT scaled by the cell area and cell depth (assuming cell depth is proportional to the break down voltage). We find that 6-mm pixel size yields worse OCT rate than 3-mm pixel size, which indicates that the major part of the OCT can propagate more than 3 mm. We also observe that LVR devices tend to have higher OCT than LCT5 and LVR2 even after taking into account the larger cell capacitance due to thinner active cell.

In order to investigate the role of the protection coating on the OCT, the OCT rate is measured for SiPMs with different coating thickness (no coating, 100 μm, 300 μm and 450 μm) as shown in Fig. 5. The lowest OCT rate is observed for the SiPM with no coating clearing indicating that the OCT is propagated via the protection coating. We also find that the OCT rate can be suppressed with thicker coating thickness when the thickness is greater than the cell size. This is because the photons that are reflected at the surface of the protection coating tend to travel longer before coming back to the SiPM cell and have may get out of the pixel boundary with thicker coating.

Fig. 6 compares the OCT rate as a function of the over voltage for the exactly same SiPMs measured at Nagoya and Catania. The OCT rate measured at Catania is systematically higher than that at Nagoya. Since the chance coincidence of two or more dark-noise counts are taken into account at the both sites, it is not the dominant origin of the difference at the both sites. We suspect that the difference is mainly due to delayed OCT where the crosstalk photon is converted in the non-depleted region and move to avalanche region by diffusion. Typical time scale of the delayed OCT is less than 20 ns [5], which can explain that the higher OCT rate is due to a longer shaping time of 15 ns at Catania.

5. PDE vs OCT rate

As described in Section 2, higher PDE at lower OCT rate is preferred in CTA. However, both PDE and OCT rate increases with higher over voltage with different over voltage dependence. Assuming the pulse shape of 10 ns FWHM, the effect of OCT becomes sub-dominant compared with the chance coincidence of 25 MHz NSB if the OCT rate is less than 5%.

Fig. 7 shows the PDE as a function of the OCT rate measured at Nagoya. This result indicates that S13360-3050CS (LVR SiPM with 50 μm cell size and 3 mm pixel size) yields the highest PDE for the OCT rate above 5% among SiPM manufactured by Hamamatsu Photonics. Since S13360-3050CS yields 5% higher PDE than any other SiPMs with scaling, this result needs further verifications.

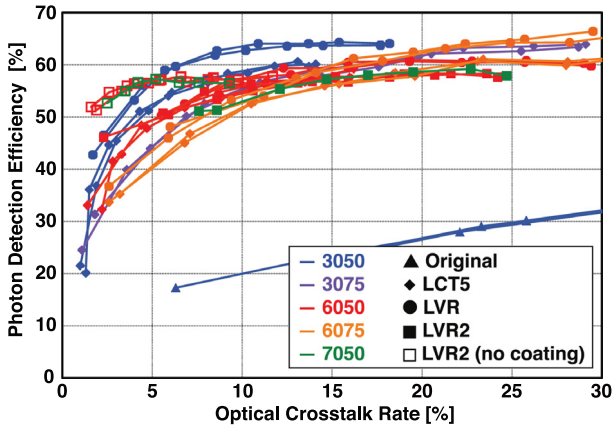

Fig. 7. PDE as a function of the OCT measured at Nagoya.

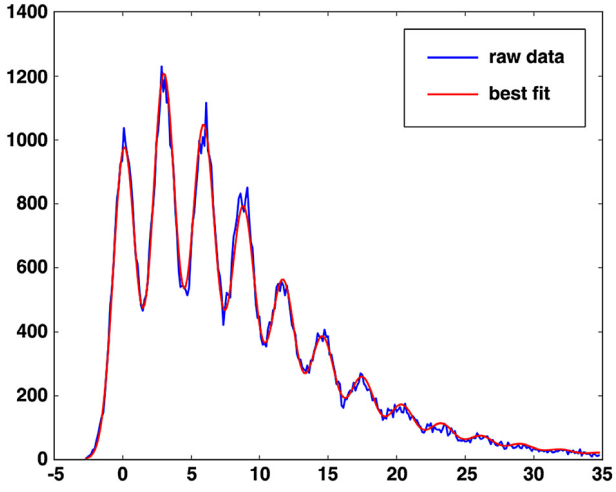

Fig. 8. Pulse height distribution of the SiPM pulse fit to a generalized Poisson distribution.

6. Mathematical modeling of SiPM pulse height distribution

We have also investigated a mathematical modeling technique to fit the SiPM pulse height distribution using the camera electronics themselves, to achieve the best possible in-situ SiPM characterization after camera installation in the telescope. Fig. 8 shows the success of fitting a Generalized Poisson distribution [6,7] to the SiPM pulse height

distribution produced from a pulsed laser input. The parameters of the fitted distribution allow the direct extraction of SiPM gain, optical crosstalk, and electronic and detector gain fluctuation characteristics.

7. Summary

We have characterized several types of SiPMs from Hamamatsu utilizing different technologies suppressing the OCT while enhancing the PDE at lower over voltage. We find that the PDE can be described very well by the fill factor and the relative over voltage and the OCT measurement depends on the shaping time of the waveform. We also find that the OCT rate can be suppressed by optimizing the thickness of the protection coating.

Acknowledgment

This work was conducted in the context of the CTA ASTRI and GCT Projects. We would like thank N. Otte and R. Mirzoyan for useful discussions. We gratefully acknowledge financial support from the agencies and organizations listed here: http://www.cta-observatory.org/consortium_acknowledgments. We also acknowledge support from JSPS/MEXT KAKENHI grant numbers 23244051, 25610040, 15H02086, 16K13801 and 17H04838.

References

[1] B.S. Acharya, M. Actis, T. Aghajani, G. Agnetta, J. Aguilar, F. Aharonian, M. Ajello, A. Akhperjanian, M. Alcubierre, J. Aleksić, et al., Introducing the CTA concept, Astropart. Phys. 43 (2013) 3–18. http://dx.doi.org/10.1016/j.astropartphys.2013.01.007.

[2] M. Actis, G. Agnetta, F. Aharonian, A. Akhperjanian, J. Aleksić, E. Aliu, D. Allan, I. Allekotte, F. Antico, L.A. Antonelli, et al., Design concepts for the cherenkov telescope array CTA: An advanced facility for ground-based high-energy gamma-ray astronomy, Exp. Astron. 32 (2011) 193–316. http://dx.doi.org/10.1007/s10686-011-9247-0. arXiv:1008.3703.

[3] T. Montaruli, G. Pareschi, T. Greenshaw, (for the CTA Consortium), The small size telescope projects for the cherenkov telescope array, in: 34th International Cosmic Ray Conference (ICRC2015), in: International Cosmic Ray Conference, 34, 2015, p. 1043 arXiv:1508.06472.

[4] G. Romeo, G. Bonanno, S. Garozzo, A. Grillo, D. Marano, M. Munari, M.C. Timpanaro, O. Catalano, S. Giarrusso, D. Impiombato, G.L. Rosa, G. Sottile, Characterization of a 6×6-mm ^{2} 75-μ m cell MPPC suitable for the cherenkov telescope array project, Nucl. Instrum. Methods A 826 (2016) 31–38. http://dx.doi.org/10.1016/j.nima.2016.04.060.

[5] A.N. Otte, G. Distefano, N. Thanh, D. Purushotham, Characterization of three high efficiency and blue sensitive silicon photomultipliers, Nucl. Instrum. Methods A 846 (2017) 106–125. http://dx.doi.org/10.1016/j.nima.2016.09.053. arXiv:1606.05186.

[6] P.C. Consul, G.C. Jain, A generalization of the poisson distribution, Technometrics 15 (1973) 791–799. http://dx.doi.org/10.2307/1267389.

[7] V. Chmill, E. Garutti, R. Klanner, M. Nitschke, J. Schwandt, On the characterisation of SiPMs from pulse-height spectra, Nucl. Instrum. Methods A 854 (2017) 70–81. http://dx.doi.org/10.1016/j.nima.2017.02.049.